

COMPARISON OF MONTE CARLO METHODS FOR NONLINEAR RADIATION TRANSPORT

William R. Martin & Forrest B. Brown
X-3 Group, Applied Physics (X) Division
Los Alamos National Laboratory
<wrm@umich.edu>, <fbrown@lanl.gov>

Keywords: Monte Carlo, radiation transport

ABSTRACT

Five Monte Carlo methods for solving the nonlinear thermal radiation transport equations are compared. The methods include the well-known Implicit Monte Carlo method (IMC) developed by Fleck and Cummings, an alternative to IMC developed by Carter and Forest, an “exact” method recently developed by Ahrens and Larsen, and two methods recently proposed by Martin and Brown. The five Monte Carlo methods are developed and applied to the radiation transport equation in a medium assuming local thermodynamic equilibrium. Conservation of energy is derived and used to define appropriate material energy update equations for each of the methods. Details of the Monte Carlo implementation are presented, both for the random walk simulation and the material energy update. Simulation results for all five methods are obtained for two infinite medium test problems and a 1-D test problem, all of which have analytical solutions. Conclusions regarding the relative merits of the various schemes are presented.

1. INTRODUCTION

The thermal radiative transfer equation describes the transport of photons in a medium that scatters and absorbs photons as well as emits photons as a result of Planckian emission due to the finite temperature of the medium. This is a nonlinear problem due to the effect of the radiation field on the temperature of the medium, which in turn affects the radiation field due to Planckian emission. Typically, Local Thermodynamic Equilibrium (LTE) is assumed, meaning that the matter is in thermal equilibrium at a temperature T , emitting photons in a Planckian spectrum (with temperature T), and the radiation field, which may be far from equilibrium, does not affect this thermal equilibrium. Solution of the nonlinear problem involves solving two equations: the radiative transfer equation with the Planckian emission source at temperature T and the energy conservation equation for the medium to obtain the temperature T .

2. EQUATIONS FOR NONLINEAR RADIATION TRANSPORT

Assuming LTE and no scattering, the radiative transfer and material energy equations may be expressed as follows [Pomraning, 1973]:

$$\frac{1}{c} \frac{\partial I(\mathbf{r}, \Omega, \nu, t)}{\partial t} + \Omega \cdot \nabla I + \sigma I = \sigma B(\nu, T) + q \quad (1)$$

$$\frac{\partial U_m(\mathbf{r}, t)}{\partial t} = \iint \sigma (I - B) d\nu d\Omega \quad (2)$$

where $I(\mathbf{r}, \Omega, \nu, t)$ is the specific radiation intensity, $U_m(\mathbf{r}, t)$ is the material energy density, $\sigma(\mathbf{r}, \nu, t)$ is the opacity (absorption only) which has been corrected for induced effects, and $B(\nu, T)$ is the Planck function describing photon emission from the material at temperature T:

$$B(\nu, T) = \frac{2h\nu^3}{c^2} \frac{1}{e^{h\nu/kT} - 1} \quad (3)$$

The material energy density, $U_m(\mathbf{r}, t)$, is related to the temperature, T, through the material equation of state. For notational convenience, the Planck function will be expressed as $B(\nu)$, suppressing the argument T. Now define the radiation energy density $E(\mathbf{r}, t)$,

$$E(\mathbf{r}, t) = \frac{1}{c} \iint I(\mathbf{r}, \nu, \Omega, t) d\nu d\Omega \quad (4)$$

and the *equilibrium* radiation energy density, $U_r(\mathbf{r}, t)$,

$$U_r(\mathbf{r}, t) = \frac{4\pi}{c} \int B(\nu, T) d\nu = aT^4 \quad (5)$$

where a is the radiation constant:

$$a = \frac{8k^4\pi^5}{15c^3h^3} \quad (6)$$

and it is noted that $E(\mathbf{r}, t) \neq U_r(\mathbf{r}, t)$ unless the radiation field is in equilibrium with the matter energy at temperature T, resulting in $I = B$.

Now express the Planckian absorption term in terms of $U_r(\mathbf{r}, t)$,

$$\sigma(\nu)B(\nu) = \frac{c}{4\pi} \sigma(\nu)b(\nu)U_r(\mathbf{r}, t) \quad (7)$$

where $b(\nu)$ is the normalized Planck spectrum

$$b(\nu) = \frac{B(\nu)}{\int B(\nu)d\nu} = \frac{15h^4\nu^3}{\pi^4k^4T^4} \frac{1}{e^{h\nu/kT} - 1} \quad (8)$$

The equilibrium radiation energy density, $U_r(\mathbf{r}, t)$, and material energy density, $U_m(\mathbf{r}, t)$, are related by

$$\frac{\partial U_m(\mathbf{r}, t)}{\partial U_r(\mathbf{r}, t)} = \frac{1}{\beta(\mathbf{r}, t)} \quad (9)$$

For a perfect gas with constant specific heat,

$$\beta(\mathbf{r}, t) = \beta(T) = \frac{4aT^4}{C_v T} = \frac{4aT^3}{C_v} \quad (10)$$

Define the Planck-weighted absorption cross-section, $\sigma_p(\mathbf{r}, t)$, as

$$\sigma_p(\mathbf{r}, t) = \int b(\nu)\sigma(\mathbf{r}, \nu, t)d\nu \quad (11)$$

Using these relations, Equations (1) and (2) may be rewritten as

$$\frac{1}{c} \frac{\partial I(\mathbf{r}, \Omega, \nu, t)}{\partial t} + \Omega \cdot \nabla I + \sigma I = \frac{c}{4\pi} \sigma b(\nu) U_r(\mathbf{r}, t) + q \quad (12)$$

$$\frac{1}{\beta(\mathbf{r}, t)} \frac{\partial U_r(\mathbf{r}, t)}{\partial t} = \iint \sigma(\nu) I(\mathbf{r}, \Omega, \nu, t) d\nu d\Omega - c \sigma_p(\mathbf{r}, t) U_r(\mathbf{r}, t) \quad (13)$$

Equation (13) may be solved directly to give:

$$U_r(\mathbf{r}, t) = U_r(\mathbf{r}, t_0) e^{-\int_{t_0}^t c\beta\sigma_p dt'} + \int_{t_0}^t dt' \beta(\mathbf{r}, t') e^{-\int_{t'}^t c\beta\sigma_p dt''} \iint I(\mathbf{r}, \Omega, \nu, t') \sigma(\nu) d\nu d\Omega \quad (14)$$

Substituting (14) into (12) gives:

$$\begin{aligned} \frac{1}{c} \frac{\partial I(\mathbf{r}, \Omega, \nu, t)}{\partial t} + \Omega \cdot \nabla I + \sigma I &= \frac{c}{4\pi} \sigma b(\nu) U_r(\mathbf{r}, t_0) e^{-\int_{t_0}^t c\beta\sigma_p dt'} \\ &+ \frac{c}{4\pi} \sigma b(\nu) \int_{t_0}^t dt' \beta(\mathbf{r}, t') e^{-\int_{t'}^t c\beta\sigma_p dt''} \iint I(\mathbf{r}, \Omega', \nu', t') \sigma(\nu') d\nu' d\Omega' + q(\mathbf{r}, \Omega, \nu, t) \end{aligned} \quad (15)$$

For the case of frequency-independent opacity, Eq. (15) becomes, upon integration over ν

$$\begin{aligned} & \frac{1}{c} \frac{\partial I(\mathbf{r}, \Omega, t)}{\partial t} + \Omega \cdot \nabla I + \sigma I \\ & = \frac{c}{4\pi} \sigma \left(U_r(\mathbf{r}, t_0) e^{-c\beta\sigma(t-t_0)} + \int_{t_0}^t dt' \beta \sigma e^{-c\beta\sigma(t-t')} \int I(\mathbf{r}, \Omega', t') d\Omega' \right) + q \end{aligned} \quad (16)$$

which is the “grey approximation” to Eq. (15).

Equation (15) or (16) represents the radiative transfer equation with explicit emission source terms representing the emission due to the initial energy distribution and all absorptions since the initial time. In the discussion that follows, Eq. (16) is solved by several Monte Carlo methods, but it should be noted that these methods may also be employed (with straightforward modifications) to solve the general frequency dependent form, Eq. (15). In each case, the derivation will be carried out with the general equation and then reduced to the special case of grey transport and constant material properties.

3. SOLUTION METHODS

For convenience, Equation (15) can be expressed:

$$\frac{1}{c} \frac{\partial I(\mathbf{r}, \Omega, \nu, t)}{\partial t} + \Omega \cdot \nabla I + \sigma I = R(\mathbf{r}, \nu, t) + S(\mathbf{r}, \nu, t) + q(\mathbf{r}, \nu, t) \quad (17)$$

where we have defined the “R” term

$$R(\mathbf{r}, \nu, t) = \frac{c}{4\pi} \sigma(\nu) b(\nu) U_r(\mathbf{r}, t_0) e^{-\int_{t_0}^t c\beta\sigma_\nu dt'} \quad (18)$$

and the “S” term,

$$S(\mathbf{r}, \nu, t) = \frac{c}{4\pi} \sigma(\nu) b(\nu) \int_{t_0}^t dt' \beta(\mathbf{r}, t') e^{-\int_{t'}^t c\beta\sigma_\nu dt''} \iint I(\mathbf{r}, \Omega', \nu', t') \sigma(\nu') d\nu' d\Omega' \quad (19)$$

The R term represents the emission due to the initial temperature distribution $U_r(\mathbf{r}, t_0)$ and the S term is the “emission integral”, representing emissions as a result of temperature changes since the initial time t_0 .

We will compare 5 different methods for solving Equation (17):

- AMC-E: the "explicit analytical Monte Carlo" method [Martin&Brown, 2001a],
- AMC-I: the "implicit analytical Monte Carlo" method [Martin& Brown, 2001a],
- CF: the method presented by Carter & Forest [Carter&Forest,1973],
- AL: the method proposed by Ahrens and Larsen [Ahrens&Larsen, 2000], and
- IMC: the traditional "implicit Monte Carlo" method [Fleck&Cumplings, 1971].

Fundamentally, these five methods differ in the approximations used to represent the R and S terms in Equation (17). They also differ in many minor implementation details, especially for computer coding, but those are not important for the present comparison. For each of the five methods, we first describe the approximations, if any, to solve Equation (17). For each of these cases, we obtain the final result assuming the grey (single frequency) approximation with constant opacities.

With this background, the essential features of the Monte Carlo implementation are described, highlighting the unique character of each approach. We assume that calculations are done in a conventional manner for a timestep beginning at time t_n and extending through time t_{n+1} . A spatial mesh is used to define the material properties, such as temperature, energy density, opacities, specific heats, etc.

The Monte Carlo calculation for a timestep begins by sampling source particles from all known source distributions, retrieving "census particles" (i.e., particles which were still active at the end of the previous timestep), and then following all particle histories until the particles are killed or reach the end of the timestep. Collision analysis differs somewhat from neutronics problems, in that particles which are absorbed may be reemitted, either immediately or after a time delay, or may be killed. Standard tallies for collision, pathlength, surface crossing, and census events are performed during the simulation of particle histories, with tally bins for each spatial mesh cell (and each frequency bin for the general case). Conventional Monte Carlo techniques such as survival biasing, stratified sampling, splitting/Russian roulette, etc., may be used for any of the Monte Carlo schemes described below where appropriate. For many Monte Carlo radiation transport codes, the particular technique of "delta scattering" [Woodcock 1965] or fictitious scattering is used to prevent large disparities in particle weights. This should be considered a code implementation detail, not an essential part of the method, since it does not alter the physics of the simulation and is generally used to improve code efficiency.

For the discussion below, all material properties are assumed to be known at the beginning of a timestep, t_n . In general, these material properties will vary continuously during a timestep, but will be assumed to be constant within a spatial mesh cell. For the simplified cases below, they are also held constant throughout the timestep. (It should be noted that most Monte Carlo codes which solve radiation transport problems have some means of modeling the variation of material properties during a timestep, generally based on an extrapolation of material properties from preceding timesteps. These are also application- and code-dependent details which are not essential to the comparison of the five schemes below.)

The right hand side of Equation (17) has three terms: R, S, and an external source q. In the discussion below, we focus on the differences in approximating and implementing the R and S terms.

3.1 AMC Explicit

The essential approximation in this method is that $I(\mathbf{r}, \Omega, \nu, t')$ in the emission integral S may be replaced by a constant, the beginning-of-timestep value $I(\mathbf{r}, \Omega, \nu, t_n)$, so that the R and S terms become

$$R(\mathbf{r}, \nu, t) = \frac{c}{4\pi} \sigma(\nu) b(\nu) U_r(\mathbf{r}, t_n) e^{-\int_n^t c\beta\sigma_p dt'} \quad (20)$$

$$S(\mathbf{r}, \nu, t) = \frac{c}{4\pi} \sigma(\nu) b(\nu) \iint I(\mathbf{r}, \Omega', \nu', t_n) \sigma(\nu') d\nu' d\Omega' \int_{t_n}^t dt' \beta(\mathbf{r}, t') e^{-\int_{t'}^t c\beta\sigma_p dt''}$$

With this approximation, the S term becomes an effective emission source, rather than an absorption-reemission term. For the special case of grey with no scattering and constant opacities, the R and S terms become

$$R(\mathbf{r}, t) = \frac{c\sigma}{4\pi} U_r(\mathbf{r}, t_n) e^{-c\beta\sigma(t-t_n)} \quad (21)$$

$$S(\mathbf{r}, t) = \frac{\sigma}{4\pi} [1 - e^{-c\beta\sigma(t-t_n)}] \int I(\mathbf{r}, \Omega, t_n) d\Omega$$

For this method, both R and S are effective sources in a Monte Carlo implementation, each with a different time dependence. The source particles generated by these two terms may be sampled at the beginning of timestep and do not affect the collision analysis performed during a timestep.

The R term is an effective source with a time variation of $e^{-c\beta\sigma(t-t_n)}$ during the timestep. The total weight of particles emitted by this source is simply $\int R(\mathbf{r}, t) dt$ for the timestep, and the time of source particle emission is sampled from a truncated exponential probability density function (PDF):

$$\tilde{t} = t_n - \frac{1}{c\beta\sigma} \ln [1 - \xi (1 - e^{-c\beta\sigma\Delta t})] \quad (22)$$

where ξ is a random number in (0,1).

The S term is an effective source with a time variation of $1 - e^{-c\beta\sigma(t-t_n)}$ during the timestep. The total weight of particles emitted by this source is simply $\int S(\mathbf{r}, t) dt$ for the timestep, and the time of source particle emission is sampled from the PDF using a rejection method [Carter-Forest, 1973]:

$$\begin{aligned}
&\text{If } 1 - e^{-\xi_1 c \beta \sigma \Delta t} > \xi_2 (1 - e^{-c \beta \sigma \Delta t}) \\
&\text{then: } \quad \text{exit with } \tilde{t} = t_n + \xi_1 \Delta t \\
&\text{otherwise: } \quad \text{repeat (with new } \xi_1, \xi_2)
\end{aligned} \tag{23}$$

For the AMC-explicit scheme, the approximation of S using the beginning of timestep intensity $I(\mathbf{r}, \Omega, \nu, t_n)$ will clearly limit the accuracy of the method, since it will not take into account variations in $I(\mathbf{r}, \Omega, \nu, t')$ during the timestep, potentially leading to a poor estimation of the emission integral S.

3.2 AMC Implicit

The essential approximation in this method is that $I(\mathbf{r}, \Omega, \nu, t')$ in the emission integral S is replaced by its instantaneous value $I(\mathbf{r}, \Omega, \nu, t)$, so that the R and S terms become

$$\begin{aligned}
R(\mathbf{r}, \nu, t) &= \frac{c}{4\pi} \sigma(\nu) b(\nu) U_r(\mathbf{r}, t_n) e^{-\int_n^t c \beta \sigma_\nu dt'} \\
S(\mathbf{r}, \nu, t) &= \frac{c}{4\pi} \sigma(\nu) b(\nu) \iint I(\mathbf{r}, \Omega', \nu', t) \sigma(\nu') d\nu' d\Omega' \int_{t_n}^t dt' \beta(\mathbf{r}, t') e^{-\int_t^{t'} c \beta \sigma_\nu dt''}
\end{aligned} \tag{24}$$

For the special case of grey with no scattering, the R and S terms simplify to:

$$\begin{aligned}
R(\mathbf{r}, t) &= \frac{c\sigma}{4\pi} U_r(\mathbf{r}, t_n) e^{-c\beta\sigma(t-t_n)} \\
S(\mathbf{r}, t) &= \frac{\sigma}{4\pi} [1 - e^{-c\beta\sigma(t-t_n)}] \int I(\mathbf{r}, \Omega, t) d\Omega
\end{aligned} \tag{25}$$

As with the AMC explicit method, the R term is an effective source representing particles emitted during the timestep due to the initial temperature. The source particles generated by this term are treated exactly as in the AMC-explicit scheme. The S term uses the instantaneous value of the intensity (i.e., at the current collision time) to model the absorption-reemission process due to collisions. Noting the similarity of S to a scattering term, we define a time-dependent effective scattering cross-section:

$$\sigma_s^{eff} = \sigma(1 - e^{-c\beta\sigma(t-t_n)}) \tag{26}$$

where t is the time of collision. Then, with probability $\sigma_s^{eff} / \sigma = 1 - e^{-c\beta\sigma(t-t_n)}$, a particle is emitted isotropically at the collision point with no time delay. This scheme for treating the S term is approximate in two regards. First, only the current collision at time t is used for modeling the absorption-reemission process at time t , rather than the collective

collisions from t_n through t that would be represented by the emission integral. Secondly, the emitted particle appears immediately without a time delay.

3.3 Carter-Forest

The R and S terms are exact during the current timestep, $t_n \leq t \leq t_{n+1}$:

$$R(\mathbf{r}, \mathbf{v}, t) = \frac{c}{4\pi} \sigma(\mathbf{v}) b(\mathbf{v}) U_r(\mathbf{r}, t_n) e^{-\int_{t_n}^t c\beta\sigma_p dt'} \quad (27)$$

$$S(\mathbf{r}, \mathbf{v}, t) = \frac{c}{4\pi} \sigma(\mathbf{v}) b(\mathbf{v}) \iint I(\mathbf{r}, \Omega', \mathbf{v}', t') \sigma(\mathbf{v}') d\mathbf{v}' d\Omega' \int_{t_n}^t dt' \beta(\mathbf{r}, t') e^{-\int_{t'}^t c\beta\sigma_p dt''}$$

For the special case of grey with no scattering, the R and S terms simplify to:

$$R(\mathbf{r}, t) = \frac{c\sigma}{4\pi} U_r(\mathbf{r}, t_n) e^{-c\beta\sigma(t-t_n)} \quad (28)$$

$$S(\mathbf{r}, t) = \frac{\sigma}{4\pi} \int_{t_n}^t dt' c\beta\sigma e^{-c\beta\sigma(t-t')} \int I(\mathbf{r}, \Omega, t') d\Omega$$

For this method, the R term is an effective source in a Monte Carlo implementation, representing particles emitted during the timestep due to the temperature at the beginning of the timestep. The source particles generated by this term are treated exactly as in the AMC-E and AMC-I schemes.

The S term accounts for all particles created by absorption-reemission from the beginning of the timestep through the current time t . The Carter-Forest approach is to treat this term exactly within the current timestep. For a collision at time t' , the contribution of emitted particles to S at time t has a distribution given by $c\beta\sigma e^{-c\beta\sigma(t-t')}$. The probability that the particle will be reemitted during the current timestep is $\int_{t'}^{t_{n+1}} c\beta\sigma e^{-c\beta\sigma(t-t')} dt = 1 - e^{-c\beta\sigma(t_{n+1}-t')}$. Thus for a collision at time t' , a time-dependent effective scattering cross-section is defined as

$$\sigma_s^{eff} = \sigma(1 - e^{-c\beta\sigma(t_{n+1}-t')}) \quad (29)$$

where t' is the time of collision. Then, with probability $\sigma_s^{eff} / \sigma = 1 - e^{-c\beta\sigma(t_{n+1}-t')}$, a particle is emitted isotropically at the collision point, but at a delayed time within the current timestep. The emission time is sampled from a truncated exponential PDF as

$$\tilde{t} = t' - \frac{1}{c\beta\sigma} \ln \left[1 - \xi \left(1 - e^{-c\beta\sigma(t_{n+1}-t')} \right) \right] \quad (30)$$

With probability $1 - \sigma_s^{eff} / \sigma$, the particle history is terminated.

The absorption-reemission events where the particle would be reemitted within the current timestep are thus treated exactly. For the cases where the particle reemission would occur at times beyond t_{n+1} , the particle is absorbed, which amounts to depositing its energy into U_r , which would result in emitting the energy via the R term at the start of the next timestep. Thus, there are no approximations in either the spatial- or time-dependence of the S term within a timestep. The only approximation in the method is that particles which would be reemitted at times beyond the current timestep are absorbed, smearing their energy throughout the cell volume (i.e., U_r is defined for a cell, not a point), so that the eventual reemission may occur at a different location within a cell than the original particle absorption. However, for the infinite medium (0-D) problem, the CF scheme is exact since there is no spatial dependence.

3.4 Ahrens-Larsen

As with the CF scheme, no approximations are made to the R and S terms. There are subtle differences between this scheme and the CF scheme. The S term includes contributions from all collisions at previous times $t > 0$, not just those collisions within the current timestep, and therefore the R term includes only the effects of the initial conditions, resulting in:

$$R(\mathbf{r}, \mathbf{v}, t) = \frac{c}{4\pi} \sigma(\mathbf{v}) b(\mathbf{v}) U_r(\mathbf{r}, 0) e^{-\int_0^t c\beta\sigma_p dt'}$$

$$S(\mathbf{r}, \mathbf{v}, t) = \frac{c}{4\pi} \sigma(\mathbf{v}) b(\mathbf{v}) \int_0^t dt' \beta(\mathbf{r}, t') e^{-\int_{t'}^t c\beta\sigma_p dt''} \iint I(\mathbf{r}, \Omega', \mathbf{v}', t') \sigma(\mathbf{v}') d\mathbf{v}' d\Omega'$$
(31)

For the special case of grey (and no scattering), the R and S terms simplify to:

$$R(\mathbf{r}, t) = \frac{c\sigma}{4\pi} U_r(\mathbf{r}, 0) e^{-c\beta\sigma t}$$

$$S(\mathbf{r}, t) = \frac{\sigma}{4\pi} \int_0^t dt' c\beta\sigma e^{-c\beta\sigma(t-t')} \int I(\mathbf{r}, \Omega, t') d\Omega$$
(32)

For this method, the R term is an effective source in a Monte Carlo implementation, representing particles emitted due to the initial material properties at the beginning of the problem. If the initial equilibrium radiation density $U_r(\mathbf{r}, t_0)$ is nonzero, the R term is evaluated at the beginning of the initial timestep; some of the generated particles would have emission times in future timesteps and would be banked until that step was analyzed. For subsequent timesteps, the R term would be zero. For these initial particles from the R term, particle emission times are sampled from an exponential PDF:

$$\tilde{t} = -\frac{1}{c\beta\sigma} \ln \xi \quad (33)$$

The S term accounts for all particles created by absorption-reemission from the beginning of the problem through the current collision time t . Unlike the Carter-Forest approach, particles emitted due to collisions are not constrained to appear within the current step; any future emission time is permitted. For a collision at time t' , the contribution of emitted particles to S at time t has a distribution given by $c\beta\sigma e^{-c\beta\sigma(t-t')}$. A particle is emitted isotropically at the collision point, but at a delayed time. If the resulting time is outside the current timestep, the particle must be banked for future analysis. The emission time is sampled from the exponential PDF as

$$\tilde{t} = t' - \frac{1}{c\beta\sigma} \ln \xi \quad (34)$$

The Ahrens-Larsen scheme treats the R and S terms exactly, with no approximations in either the time- or spatial-dependence. It should be noted that the method outlined above applies for the case of time-independent material properties (e.g., σ, β). If the material properties change from one timestep to the next, the method must be revised, for instance to resample emission times for banked particles from Eq. (33) at the start of each timestep using the new material properties. It should also be noted that the principal challenge in effectively implementing the Ahrens-Larsen method is managing a potentially very large number of particles: Particles are not killed at collisions, so the number of particles in the simulation grows as additional source particles are created. That is, every particle created in the problem remains throughout the entire calculation. Some means of population control is essential, through standard techniques such as stratified sampling (a.k.a., "combing") or Russian roulette. Care must be taken, however, to ensure that energy is conserved whenever the particle population is reduced.

3.5 Fleck-Cummings, IMC

The derivation of the IMC equations will be briefly summarized. There are two distinct approximations which are made. First, the instantaneous equilibrium radiation energy density at the current time is approximated as a linear combination of beginning and end of timestep values,

$$U_r(\mathbf{r}, t) = \alpha U_r(\mathbf{r}, t_{n+1}) + (1 - \alpha) U_r(\mathbf{r}, t_n) \quad (35)$$

where $0 \leq \alpha \leq 1$. The energy equation (13) is then integrated over the timestep, yielding an expression for the emission integral in terms of $U_r(\mathbf{r}, t_n)$ and $U_r(\mathbf{r}, t_{n+1})$. Equation (35) is then used to eliminate $U_r(\mathbf{r}, t_{n+1})$ and the resultant expression for the emission integral is substituted back into the radiative transfer equation (12). At this point the second, and most important, approximation is made: $I(\mathbf{r}, \Omega, \mathbf{v}, t')$ in the emission integral is replaced by its instantaneous value, $I(\mathbf{r}, \Omega, \mathbf{v}, t)$, as in the AMC implicit scheme. This results in

an approximate form of the radiative transport equation with two terms on the right hand side which correspond exactly to the R and S terms:

$$R(\mathbf{r}, \nu, t) = f \frac{c}{4\pi} \sigma(\nu) b(\nu) U_r(\mathbf{r}, t_n) \quad (36)$$

$$S(\mathbf{r}, \nu, t) = (1-f) \frac{1}{4\pi} \frac{\sigma(\nu) b(\nu)}{\sigma_p} \iint I(\mathbf{r}, \Omega', \nu', t) \sigma(\nu') d\nu' d\Omega'$$

where we have defined

$$f = \frac{1}{1 + \alpha c \beta \sigma_p \Delta t} \quad (37)$$

The parameter α must be in the range $[0,1]$ and may vary from one timestep to the next and represents the degree of "implicitness" in the method (although material properties such as σ and β are assumed to be constant at their beginning of timestep values). Values in the range 0.5-1.0 are typically chosen in practice.

For the special case of grey with no scattering, the R and S terms simplify to:

$$R(\mathbf{r}, t) = \frac{c\sigma}{4\pi} U_r(\mathbf{r}, t_n) \cdot f \quad (38)$$

$$S(\mathbf{r}, t) = \frac{\sigma}{4\pi} (1-f) \int I(\mathbf{r}, \Omega, t) d\Omega$$

For this method, the R term is an effective source in a Monte Carlo implementation, representing particles uniformly emitted during the timestep due to the temperature at the beginning of the timestep. The total weight of particles emitted by this source is simply $\int R(\mathbf{r}, t) dt$ for the timestep, and the time of source particle emission is sampled as:

$$\tilde{t} = t_n + \xi \Delta t \quad (39)$$

The S term uses the instantaneous value of the intensity (i.e., at the current collision time) to model the absorption-reemission process due to collisions. As with the AMC implicit scheme, we can define an effective scattering cross-section:

$$\sigma_s^{eff} = (1-f)\sigma \quad (40)$$

Then, with probability $\sigma_s^{eff} / \sigma = 1-f$, a particle is emitted isotropically at the collision point with no time delay. With probability f , the particle is absorbed. This scheme for treating the S term is approximate in that only the current collision at time t is used for

modeling the absorption-reemission process, rather than the collective collisions from t_n through t , and the particle is emitted immediately. While there are superficial similarities between the IMC and implicit AMC schemes, the differences are substantial. In particular, the IMC scheme scatters and emits particles uniformly in time throughout the timestep, while these are both time-dependent processes with the implicit AMC scheme.

3.6 Conservation of Energy

An expression for overall energy balance (radiation energy plus material energy) will now be obtained. First, integrate Eq. (12) over angle and frequency:

$$\frac{\partial E(\mathbf{r}, t)}{\partial t} + \nabla \cdot \vec{F} + \iint \sigma(\nu) I(\mathbf{r}, \Omega, \nu, t) d\nu d\Omega = c\sigma_p U_r(\mathbf{r}, t) + Q(\mathbf{r}, t) \quad (41)$$

where $E(\mathbf{r}, t)$ is the radiation energy density, $\vec{F}(\mathbf{r}, t)$ is the radiative flux of energy, and $Q(\mathbf{r}, t)$ is the external energy source:

$$\begin{aligned} E(\mathbf{r}, t) &= \frac{1}{c} \iint \mathbf{I}(\mathbf{r}, \Omega, \nu, t) d\Omega d\nu \\ \vec{F}(\mathbf{r}, t) &= \iint \mathbf{I}(\mathbf{r}, \Omega, \nu, t) \Omega d\Omega d\nu \\ Q(\mathbf{r}, t) &= \iint \mathbf{q}(\mathbf{r}, \Omega, \nu, t) d\Omega d\nu \end{aligned}$$

Now add Eqs. (13) and (41) to obtain:

$$\frac{\partial E(\mathbf{r}, t)}{\partial t} + \frac{1}{\beta(\mathbf{r}, t)} \frac{\partial U_r(\mathbf{r}, t)}{\partial t} + \nabla \cdot \vec{F} = Q(\mathbf{r}, t) \quad (42)$$

Expressing Eq. (42) in terms of the matter energy density and combining terms, we have:

$$\frac{\partial (E + U_m)}{\partial t} = Q(\mathbf{r}, t) - \nabla \cdot \vec{F} \quad (43)$$

which is the statement of conservation of total energy (radiation plus matter): the time rate of change of the total energy is the source strength minus the leakage. To implement Eq. (43) in a Monte Carlo code, integrate Eq. (43) over a spatial domain R (e.g., a cell) and then integrate that expression over time to obtain:

$$[\mathcal{T}(t_n) - \mathcal{T}(t_0)] + [M(t_n) - M(t_0)] = \int_{t_0}^{t_n} Q(t) dt - \int_{t_0}^{t_n} L(t) dt \quad (44)$$

where the following terms are defined:

$$\begin{aligned}
\mathcal{T}(t) &= \int_R E(\mathbf{r}, t) d\mathbf{r} && \text{"radiation energy at time } t\text{"} \\
\mathcal{M}(t) &= \int_R U_m(\mathbf{r}, t) d\mathbf{r} && \text{"total material energy at time } t\text{"} \\
\mathcal{Q}(t) &= \int_R Q(\mathbf{r}, t) d\mathbf{r} && \text{"total source energy at time } t\text{"} \\
\mathcal{L}(t) &= \int_R \nabla \cdot \vec{F} d\mathbf{r} && \text{"net energy leakage at time } t\text{"}
\end{aligned}$$

Equation (44) expresses the simple statement that the change in the radiation energy plus the change in the material energy must equal the total source energy minus the net energy leakage. All of these quantities are easily tallied with conventional Monte Carlo techniques. It is easy to show that all of the five Monte Carlo methods described above satisfy Eq. (44) exactly if analog estimators are used for all tallies and the temperature updates are performed consistently with these tallies. This is discussed in the following section.

3.7 Material Energy Update

This section describes the methodology for updating the material energy density at the end of the timestep. Solve Eq. (41) for $\partial E / \partial t$ and substitute into Eq. (43):

$$\frac{\partial U_m(\mathbf{r}, t)}{\partial t} = \iint \sigma(\nu) I(\mathbf{r}, \Omega, \nu, t) d\nu d\Omega - c\sigma_p U_r(\mathbf{r}, t) \quad (45)$$

Equation (45) represents conservation of material energy and is simply the difference between the absorption and emission rates. Noting that the five Monte Carlo methods differ only in their treatment of the emission term $c\sigma_p U_r(\mathbf{r}, t)$,

$$c\sigma_p U_r(\mathbf{r}, t) \approx \iint [R(\mathbf{r}, \nu, t) + S(\mathbf{r}, \nu, t)] d\Omega d\nu \quad (46)$$

we can express Eq. (45) in terms of the actual R and S terms used for each method:

$$\frac{\partial U_m(\mathbf{r}, t)}{\partial t} = \iint \sigma(\nu) I(\mathbf{r}, \Omega, \nu, t) d\nu d\Omega - \iint [R(\mathbf{r}, \nu, t) + S(\mathbf{r}, \nu, t)] d\Omega d\nu \quad (47)$$

Now integrate Eq. (47) over the timestep to obtain the updated material energy density at the end of the timestep:

$$\begin{aligned}
U_m(\mathbf{r}, t_{n+1}) &= U_m(\mathbf{r}, t_n) + \int_{t_n}^{t_{n+1}} \iint \sigma(\nu) I(\mathbf{r}, \Omega, \nu, t) d\nu d\Omega dt \\
&\quad - \int_{t_n}^{t_{n+1}} \iint [R(\mathbf{r}, \nu, t) + S(\mathbf{r}, \nu, t)] d\Omega d\nu dt
\end{aligned} \quad (48)$$

In practice, Eq. (48) would be integrated over a spatial cell to obtain the updated material energy for that cell.

The following sections present the expressions for the updated material density for each of the five methods assuming the special case of grey and constant opacities.

Explicit AMC

Substituting the expressions for R and S from Section 3.1 into Eq. (48) and integrating, we find:

$$U_m(\mathbf{r}, t_{n+1}) = U_m(\mathbf{r}, t_n) + \int_{t_n}^{t_{n+1}} \sigma \Phi(\mathbf{r}, t) dt - \frac{U_r(\mathbf{r}, t_n)}{\beta} (1 - e^{-c\beta\sigma\Delta t}) - c\Phi_n \Delta t + \frac{\Phi_n}{c\beta} (1 - e^{-c\beta\sigma\Delta t}) \quad (49)$$

where $\Phi(\mathbf{r}, t) = \iint \mathbf{I}(\mathbf{r}, \Omega, \nu, t) d\Omega d\nu$ is the integrated intensity and $\Phi_n = \Phi(\mathbf{r}, t_n)$. Given the definition of the R and S terms from Section 3.1, Eq. (49) can be expressed in words as

$$U_m(\mathbf{r}, t_{n+1}) = U_m(\mathbf{r}, t_n) + \# \text{ absorptions} - \# \text{ emissions}$$

hence each absorption/emission results in an energy gain/loss to the material as a result of the energy carried by each photon bundle. For explicit AMC, the emission terms are known quantities at t_n . Therefore, if the analog collision estimator is used to estimate the absorption and emission rates, energy will be *exactly* conserved by the Monte Carlo simulation. If alternative techniques are used to estimate the absorption rate or other terms in Eq. (49), then energy conservation will be satisfied in only a statistical sense. In practice, we have observed with our test problems somewhat better results when analog estimators are used to update the material energy. This assumes consistency between the solutions of the radiation transport equation and the material energy update step, and may be important for maintaining conservation of energy throughout the simulation.

Implicit AMC

Substituting the expressions for R and S from Section 3.2 into Eq. (48) and integrating, we find:

$$U_m(\mathbf{r}, t_{n+1}) = U_m(\mathbf{r}, t_n) + \int_{t_n}^{t_{n+1}} \sigma \Phi(\mathbf{r}, t) dt - \frac{U_r(\mathbf{r}, t_n)}{\beta} (1 - e^{-c\beta\sigma\Delta t}) - \int_{t_n}^{t_{n+1}} \sigma (1 - e^{-c\beta\sigma(t-t_n)}) \Phi(\mathbf{r}, t) dt \quad (50)$$

The R term is identical to its use in the explicit AMC method. Using the definition of the effective scattering cross section from Eq. (26), we can express Eq. (50) in words:

$$U_m(\mathbf{r}, t_{n+1}) = U_m(\mathbf{r}, t_n) + \#collisions - \#emissions - \#scatters$$

In this case, the scatters are effective emissions, which is the essence of the implicit AMC method. Again, the use of analog estimators for the collision, emission, and scattering rates will ensure exact energy conservation for implicit AMC.

Carter-Forest method

Substituting the expressions for R and S from Section 3.3 into Eq. (48) and integrating, we find:

$$U_m(\mathbf{r}, t_{n+1}) = U_m(\mathbf{r}, t_n) + \int_{t_n}^{t_{n+1}} \sigma \Phi(\mathbf{r}, t) dt - \frac{U_r(\mathbf{r}, t_n)}{\beta} (1 - e^{-c\beta\sigma\Delta t}) - \int_{t_n}^{t_{n+1}} \sigma (1 - e^{-c\beta\sigma(t_{n+1}-t)}) \Phi(\mathbf{r}, t) dt \quad (51)$$

where we have used the fact that S(t) is defined during the current timestep. Using the definition of the effective scattering cross section from Eq. (29), we can express Eq. (51) in the following words:

$$U_m(\mathbf{r}, t_{n+1}) = U_m(\mathbf{r}, t_n) + \#collisions - \#emissions - \#scatters$$

Ahrens-Larsen method

Substituting the *exact* (for all time) expressions for R and S from Section 3.4 into Eq. (48) and integrating from $t = 0$ to t , we find:

$$U_m(\mathbf{r}, t) = U_m(\mathbf{r}, 0) + \int_{t_n}^{t_{n+1}} \sigma \Phi(\mathbf{r}, t) dt - \int_0^t dt' c \sigma \int_0^{t'} \beta e^{-c\beta\sigma(t'-t'')} \sigma \Phi(\mathbf{r}, t'') dt'' \quad (52)$$

where we have used the fact that S(t) is defined during the current timestep. Following the analysis in Section 3.4, Eq. (52) may be interpreted as:

$$U_m(\mathbf{r}, t_{n+1}) = U_m(\mathbf{r}, t_n) + \#absorptions - \#emissions$$

and again energy is conserved exactly in this analog scheme to update the material energy density.

IMC (Fleck and Cummings)

Substituting Eq. (38) into Eq. (48) and integrating, we find:

$$U_m(\mathbf{r}, t_{n+1}) = U_m(\mathbf{r}, t_n) + \int_{t_n}^{t_{n+1}} \sigma \Phi(\mathbf{r}, t) dt - fc\sigma U_r(\mathbf{r}, t_n) - \int_{t_n}^{t_{n+1}} \sigma(1-f)\Phi(\mathbf{r}, t) dt \quad (53)$$

Since the effective scattering cross section is $\sigma(1-f)$, we can express Eq. (53) as follows:

$$U_m(\mathbf{r}, t_{n+1}) = U_m(\mathbf{r}, t_n) + \#collisions - \#emissions - \#scatters$$

As with the implicit AMC and CF methods, the scatters are effective emissions and the use of analog estimators for the collision and scattering rates will assure exact energy conservation for IMC.

4. NUMERICAL RESULTS

4.1 Monte Carlo Code Description

A 3D computer code was developed to solve the nonlinear radiative transfer equations using any of the 5 solution methods described in Section 3 – AMCE, AMCI, CF, AL, IMC. All 5 methods were implemented using the same underlying code framework, to permit a consistent comparison of accuracy, running times, and other computational considerations. The underlying code was written in C++ using the Metrowerks Codewarrior compiler and run on a 500-MHz Pentium-III processor, with 320 MB of memory (more than sufficient to ensure no swapping for the test problems).

The code uses an XYZ mesh with arbitrary mesh spacings, with material properties assumed constant within each mesh cell for the duration of a timestep. A full set of tallies is provided for each timestep, including pathlength, collision, and census tallies for the cell-averaged radiation intensities; cell tallies for the source and emission (R and S terms); surface tallies of the radiation intensities for every cell surface; tallies of the net leakage for each cell; for the Ahrens-Larsen method, special census tallies of the radiation intensity and equilibrium radiation energy density for each cell; and various other quantities of interest. For comparison with analytic results, routines are provided to interpolate cell-averaged tallies to selected edit points in space. A simple timestep controller provides for either constant or varying timestep sizes, which are adjusted if needed to provide edits at specified points in time.

The 5 solution methods affect the coding of only the collision analysis and the R and S emission terms. Four of the methods – AMCE, AMCI, CF, IMC – were implemented such that they may be combined in any proportion. This capability was indeed used to investigate combining the AMCE and AMCI methods, with some success for the infinite medium problems discussed below. In general, analog Monte Carlo techniques were used whenever possible. This was done to avoid complicating the comparison of the 5 methods. (In addition, investigating the correctness and effectiveness of "standard" variance reduction techniques applied to nonlinear time-dependent problems is a major effort.) The one exception is the use of stratified sampling to control the overall particle population at the start of each timestep. After introducing the census particles (those particles still active at the end of the previous step) and the source particles from the Q,

R, and S terms for a timestep, stratified sampling is used if necessary to reduce the number of active particles to a pre-specified number. This technique preserves the total particle weight exactly and results in uniform particle weights for a timestep. Such techniques as survival biasing, splitting, and Russian roulette were not used, and all tallies were made in an analog fashion. Material energy updates were made using analog estimators of the collision and emission rates in each cell, according to Eq. (48). (For the AL method, radiation energy density was estimated directly using the "delayed" particles in the particle bank.) For consistency in comparing the methods, material properties for a timestep were not extrapolated from previous timestep values.

4.2 Infinite Medium Problems

Two test problems with analytical solutions have been created and solved with our Monte Carlo codes. Both test problems are based on the "assume a solution, calculate the source" methodology, which has been used successfully in many areas to provide a rigorous verification check for a computational method.

The first test problem is based on an assumed linear dependence of the equilibrium radiation energy density on time, $U_r(t) = \lambda t$, which leads to the flux solution $\Phi(t) = (\lambda / \Sigma) + \lambda t$ and the desired source $Q(t) = Q_0 = 2\lambda$. The Monte Carlo code was then run with this constant source and initial conditions $\Phi(0) = \lambda / \Sigma$ and $U_r(0) = 0$. For this case, we used $\lambda = 5$ and $\beta = c = \Sigma = 1$.

The second test problem assumes an exponential form for the temperature, $U_r(t) = 1 - e^{-\lambda t}$, which leads to $\Phi(t) = 1 + \lambda(-1 + \lambda / \Sigma)e^{-\lambda t}$ and $Q(t) = \lambda(2 - \lambda / \Sigma)e^{-\lambda t}$. The Monte Carlo simulation is then performed by sampling from this $Q(t)$ source distribution with initial conditions $\Phi(0) = \lambda / \Sigma$ and $U_r(0) = 0$. In order to maintain $Q(t) > 0$ and $\Phi(t) > 0$ during the simulation, we need to restrict $\Sigma < \lambda < 2\Sigma$. For this case, we used $\lambda = 1.5$ and $\beta = c = \Sigma = 1$.

Results for the two infinite medium problems were reported earlier [Martin-Brown, 2001] and included detailed comparison of the simulation and reference results. The 3D Monte Carlo code was used to repeat the infinite medium problems, using a single mesh cell with reflective boundaries at $x, y, z = \pm 100$. This exercised the collision analysis and emission source routines in the 3D code. Results for the infinite medium test problems #1 and #2, using 250,000 source particles and fixed timesteps of $\Delta t = 0.1, 1.0, 10.0$, matched those previously run with an infinite medium code. Relative RMS errors averaged over all timesteps for these cases are shown in Table (1). The results indicate that all methods give comparable accuracy for fine timesteps ($\Delta t = 0.1$). For medium sized timesteps ($\Delta t = 1$), AL, IMC($\alpha = 0.5$), and a mix of 25% AMCE + 75% AMCI are the most accurate. For very large timesteps ($\Delta t = 10$), the AL and IMC($\alpha = 0.5$) methods are the most accurate. As noted in Section 3, we consider the AL method to be exact, except for statistical fluctuations, since there are no approximations made to Eq (17). The IMC

method does remarkably well, given the proper choice of α , considering the various approximations that it involves.

4.3 Su-Olson Benchmark Problem

Su and Olson have provided an analytical benchmark for the non-equilibrium radiative transfer problem in an isotropically scattering medium [Su-Olson, 1997]. The problem consists of a cold, infinite, homogeneous slab with a unit radiation source in $|x| < .5$ for times $0 < t < 10$, with $\sigma = \beta = c = 1$. Analytic solutions (based on the transport equation, not diffusion) are provided at 15 points logarithmically spaced in $0.1 < x < 20$ and for times $t = 0.1, 0.312, 1.0, 3.12, 10.0, 31.2, 100$. We present here only the results for $\sigma_s = 0$.

Figure (1) shows the radiation intensity for various times for the solutions obtained with all 5 methods, and Figure (2) shows the associated equilibrium radiation energy density. These cases were run using fine timesteps, varying from $\Delta t = 0.005$ to 1.0 as indicated in the figures, to demonstrate that all 5 solution methods would yield accurate results using small timesteps. The relative RMS errors in spatial values are listed in Table (2) at specified times for each of the 5 methods. The relatively large errors for the first 1 or 2 times are primarily statistical, since there are very few source particles generated in the small time interval $t < 0.3$. All methods give comparable accuracy using fine timesteps; differences in Table (2) are largely statistical, as can be seen from examining Figures (1) and (2).

Figure (3) and Table (3) give results for the Su-Olson problem run with coarse timesteps. The initial timesteps are $\Delta t = .1, .212, .688, 2.12, 5, 1.88$ in order to provide results at the Su-Olson times for analytic results, and then $\Delta t = 5$ is used for the remainder of the calculation. For $t < 1$, all methods give good agreement and are comparable in accuracy. At times $t > 1$, relatively large errors arise for the AMCE method. The errors in AMCE are expected for large timesteps, considering the approximations made to the emission term S . As expected, AL is consistently more accurate, and the AL errors are indicative of the statistical fluctuations. CF, AMCI, and IMC($\alpha = .5$) all do well for the larger timesteps, with accuracy comparable to AL.

5. CONCLUSIONS

We have examined 5 different Monte Carlo methods for solving the radiative transfer equations, comparing the different approximations made to the underlying equations, the different approaches to implementing the Monte Carlo solution techniques, and the accuracy for 3 benchmark problems for a variety of timestep sizes. Based on this work, we conclude:

- The Ahrens-Larsen method makes no approximations to the underlying equations, is potentially exact in treating the time- and space-dependence, and consistently produces the most reliable and accurate results. The method is new and requires further development in order to treat difficult, realistic problems, but is extremely promising since it retains high accuracy independent of the timestep size.

- The Carter-Forest method yields essentially the same results as the Ahrens-Larsen method, with minor differences in errors that are due to statistical variations, especially for the Su-Olson test problem early in the transient when there are few particles present. Since this method is exact within a timestep and is just as easy to implement as IMC, this method has potential as an "improved IMC", which does not require arbitrary parameters.
- The Fleck-Cummings IMC method does very well on the test problems, producing accurate results so long as the adjustable parameter α is chosen properly. This is remarkable, given that several significant approximations are made to the underlying equations. The method has been used for 30 years and is well-proven to be robust.
- The Martin-Brown AMC-implicit method also does very well on the test problems, producing accurate results without the use of ad hoc factors and with no increase in computing time compared to IMC. However, we see no reason to pursue further development of AMC-implicit or other schemes that attempt to approximate the emission integral $S(t)$, since the Carter-Forest scheme makes no approximations and is just as easy to implement.
- The Martin-Brown AMC-explicit method loses accuracy when large timesteps are used, as expected based on the approximations involved. While there is some chance that a combined AMCI-AMCE method could provide improved accuracy, much like the Fleck-Cummings α -weighting, our initial experience indicates that the accuracy of AMCE degrades too much for this to happen when large timesteps are used.
- All 5 of the methods are accurate and produce correct solutions if timesteps are chosen sufficiently small.

Based on the comparison we have made with our test problems, we recommend that further effort to solve the radiation transport equations with Monte Carlo focus on the "exact" schemes, Carter-Forest and Ahrens-Larsen. With regards to these two methods, the Ahrens-Larsen scheme preserves the exact equations for all time whereas the Carter-Forest scheme is only exact within a timestep. However, the Carter-Forest scheme could be easily implemented because there are only two changes that need to be made to an IMC code: (1) the scattering probability is time-dependent and (2) the initial emission source is time-dependent. However, we hasten to add that an important test of these methods are more realistic test problems with material properties that are both time- and space-dependent, resulting in nonlinear feedback effects that will provide a more stringent test of these methods than our current suite of linear test problems.

NOMENCLATURE

$I(\mathbf{r}, \Omega, \nu, t)$	specific radiation intensity
$E(\mathbf{r}, t)$	radiation energy density
$\Phi(\mathbf{r}, t)$	integrated radiation intensity
$\vec{F}(\mathbf{r}, t)$	radiative flux of energy
$U_r(\mathbf{r}, t)$	equilibrium radiation energy density

$U_m(\mathbf{r},t)$	material energy density
$Q(\mathbf{r},t)$	external source of radiation energy
$B(\nu,T)$	Planck function
$b(\nu)$	normalized Planck spectrum
$\sigma_p(\mathbf{r},t)$	Planck-weighted absorption cross section
$R(\mathbf{r},\nu,t)$	emission term
$S(\mathbf{r},\nu,t)$	emission term

REFERENCES

Ahrens, C., & Larsen, E.W., "An Exact Monte Carlo Method for Linear Radiative Transfer Problems," *Trans. Am. Nucl. Soc.* **83**, 340-341 (November 2000).

Ahrens, C., & Larsen, E.W., "A Semi-analog Monte Carlo Method for Grey Radiative Transfer Problems", Proceedings ANS Mathematics and Computations Topical Meeting, Salt Lake City (Sept 2001).

Carter, L.L., Cashwell, E.D., & Taylor, W.M., "Monte Carlo Sampling with Continuously Varying Cross Sections Along Flight Paths", *Nucl. Sci. Eng.* **48**, 403-411 (1972).

Carter, L.L., & Forest, C.A., "Nonlinear Radiation Transport Simulation with an Implicit Monte Carlo Method," LA-5038, Los Alamos National Laboratory (1973).

Everett, C.J., & Cashwell, E.D. , "A Third Monte Carlo Sampler", Los Alamos National Laboratory report, LA-9721-MS (March, 1983).

Fleck, J.A. Jr., & Cummings, J.D., An Implicit Monte Carlo Scheme for Calculating Time and Frequency Dependent Nonlinear Radiation Transport," *J. Comp. Phys.* **8**, 313-342 (1971).

Martin, W.R., & Brown, F.B., "The Analytical Monte Carlo Method for Radiation Transport Calculations", *Trans. Am. Nucl. Soc.* (June, 2001).

Pomraning, G.C., The Equations of Radiation Hydrodynamics, Pergamon, Oxford (1973).

Su, B., and Olson, G.L., "An Analytical Benchmark for Non-equilibrium Radiative Transfer in an isotropically Scattering Medium", *Ann. Nucl. Energy*, Vol. 24, No. 13, pp. 1035-1055 (1997).

Woodcock, E.R., et al, "Techniques Used in the GEM Code...", Proc. Conf. Application of Computing Methods to Reactor Physics Delta tracking, ANL-7050 (May, 1965).

Table 1. Relative RMS errors for infinite medium problems

Infinite Medium Problem #1									
	Relative RMS Error in I (%)			Relative RMS Error in Ur (%)			CPU Time (s)		
	t0=0, t1=1, Δt=.1	t0=0, t1=10, Δt=1	t0=0, t1=100, Δt=10	t0=0, t1=1, Δt=.1	t0=0, t1=10, Δt=1	t0=0, t1=100, Δt=10	t0=0, t1=1, Δt=.1	t0=0, t1=10, Δt=1	t0=0, t1=100, Δt=10
AMCE	0.052	1.3	18.	0.15	1.6	19.	52	41	93
AMCI	0.028	0.49	3.5	0.078	0.57	3.6	51	37	61
.5E+.5I	0.032	0.52	12.	0.088	0.61	12.	51	41	84
.25E+.75I	0.033	0.097	5.8	0.093	0.11	5.9	51	40	74
CF	0.013	0.055	0.033	0.036	0.065	0.034	48	37	61
AL	0.023	0.090	0.11	0.063	0.11	0.11	53	37	55
IMC,α=.5	0.037	0.094	0.41	0.10	0.11	0.42	52	38	65
IMC,α=.75	0.15	0.50	0.47	0.43	0.59	0.48	52	38	63
IMC,α=1.0	0.31	1.1	1.3	0.86	1.3	1.3	52	37	58
Infinite Medium Problem #2									
	Relative RMS Error in I (%)			Relative RMS Error in Ur (%)			CPU Time (s)		
	t0=0, t1=1, Δt=.1	t0=0, t1=10, Δt=1	t0=0, t1=100, Δt=10	t0=0, t1=1, Δt=.1	t0=0, t1=10, Δt=1	t0=0, t1=100, Δt=10	t0=0, t1=1, Δt=.1	t0=0, t1=10, Δt=1	t0=0, t1=100, Δt=10
AMCE	0.047	0.82	8.3	0.11	0.86	8.3	59	38	142
AMCI	0.074	0.37	1.7	0.18	0.39	1.7	63	31	45
.5E+.5I	0.041	0.25	6.5	0.097	0.26	6.5	62	35	96
.25E+.75I	0.015	0.13	4.5	0.034	0.14	4.5	62	34	79
CF	0.045	0.071	0.067	0.11	0.075	0.067	71	113	181
AL	0.015	0.048	0.080	0.036	0.050	0.080	64	31	42
IMC,α=.5	0.019	0.81	7.8	0.046	0.85	7.8	63	32	54
IMC,α=.75	0.14	0.11	4.0	0.34	0.11	4.0	63	31	47
IMC,α=1.0	0.35	0.91	1.8	0.82	0.95	1.8	63	29	43

Table 2. Relative RMS errors for Su-Olson problem, variable timesteps, 100,000 source particles, 200 cells

Time	Relative RMS Error in I (%)					Relative RMS Error in Ur (%)				
	AMCE	AMCI	CF	AL	IMC,α=.5	AMCE	AMCI	CF	AL	IMC,α=.5
0.1	1.9	2.6	1.2	1.7	1.7	9.3	15.	18.	9.9	11.
0.316	2.2	1.4	1.1	0.57	1.2	3.9	3.3	2.0	5.1	3.9
1.0	1.4	1.5	2.6	0.93	1.4	0.95	1.3	1.9	1.8	1.1
3.16	0.93	0.77	0.62	0.63	0.36	0.80	0.51	0.70	0.60	0.48
10.0	0.55	0.58	0.94	0.58	0.90	0.41	0.48	0.25	0.43	0.65
31.6	0.62	0.42	0.91	0.72	0.72	0.74	0.70	0.58	0.88	0.48
100.0	0.89	0.93	1.2	1.2	0.54	1.3	0.99	0.95	1.4	0.78
CPU time	404 s	339 s	323 s	343 s	346 s					

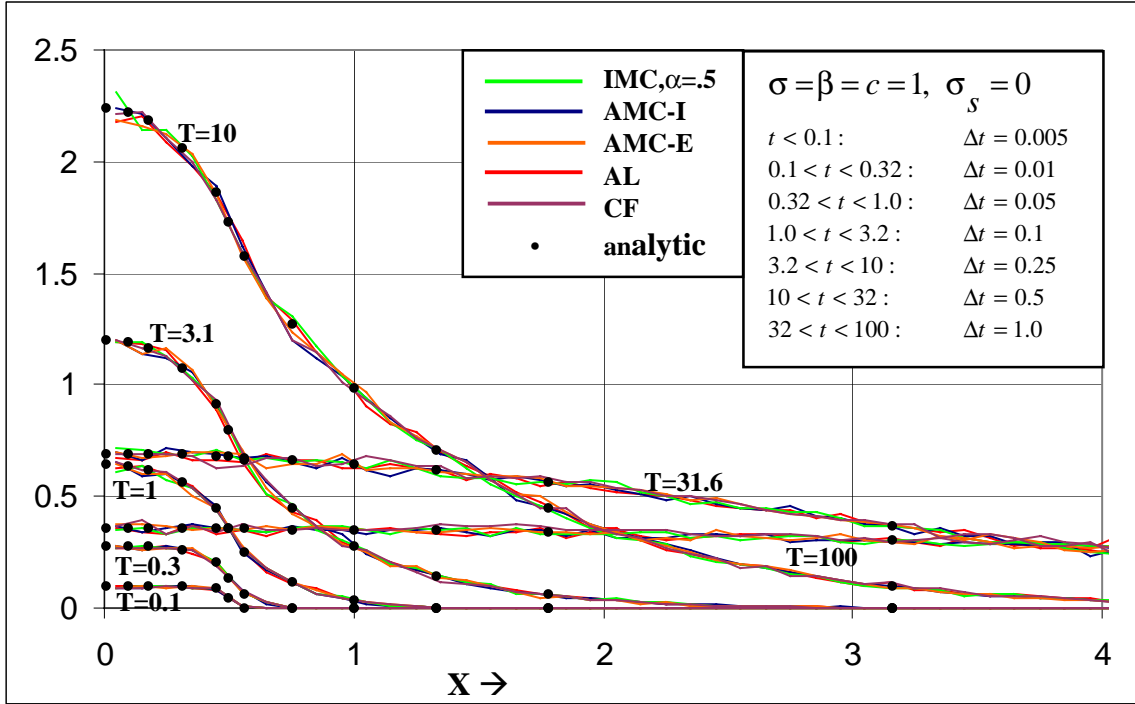


Figure 1. Integrated Radiation Intensity, $\int I d\Omega$, for Su-Olson problem, variable timesteps, 100,000 source particles, 200 cells

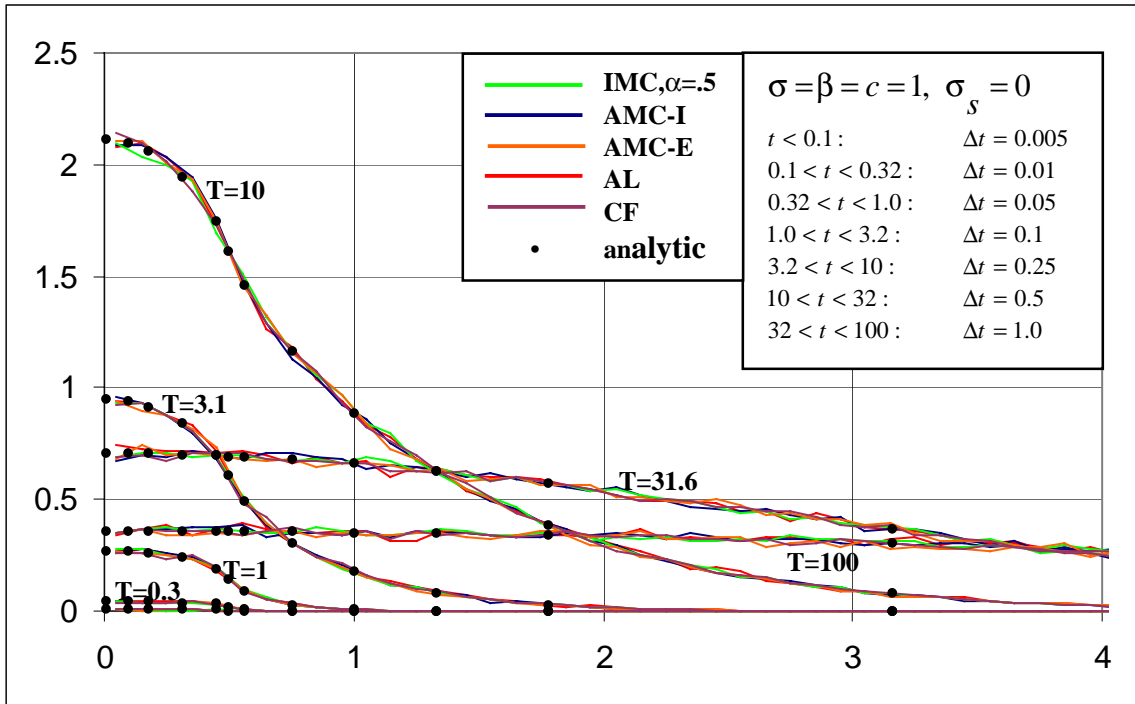


Figure 2 Equilibrium Radiation Energy Density, U_r , for Su-Olson problem, variable timesteps, 100,000 source particles, 200 cells

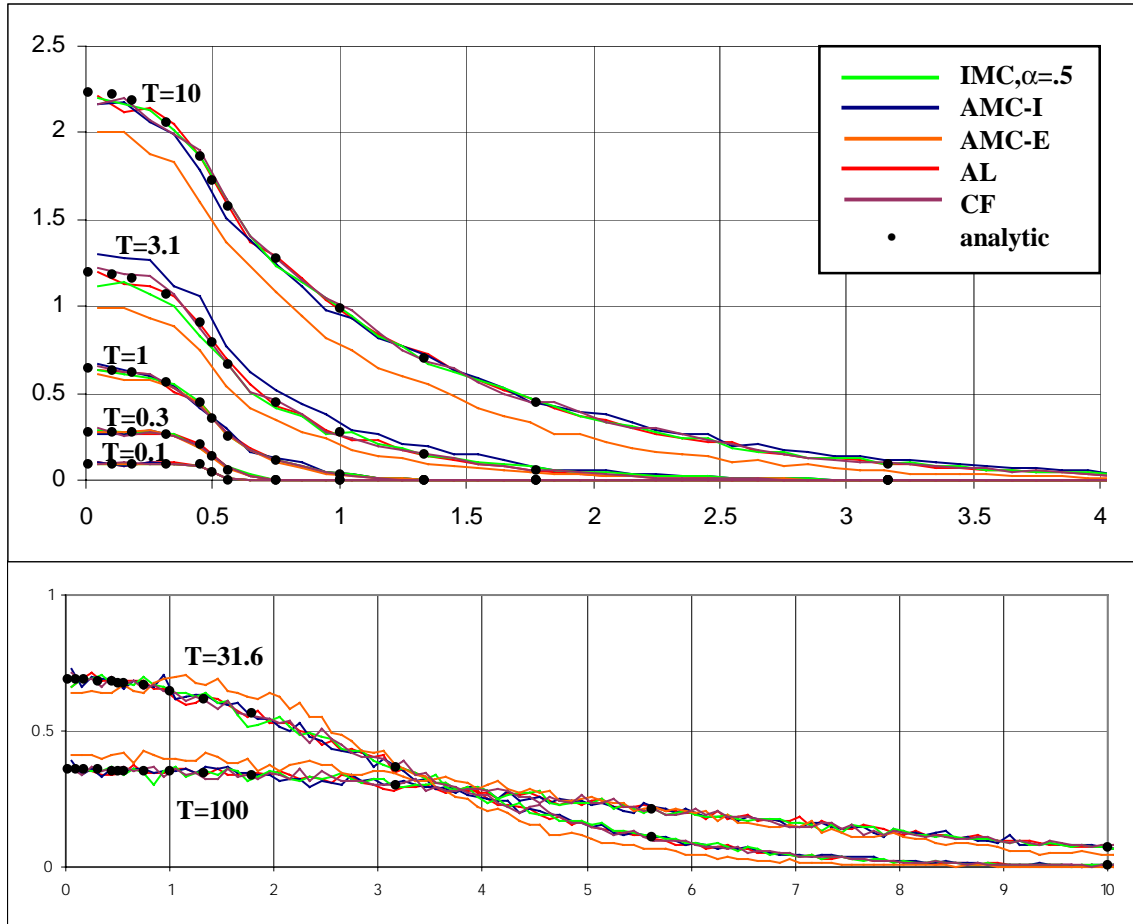


Figure 3. Integrated Radiation Intensity, $\int I d\Omega$, for Su-Olson problem, coarse timesteps, $\Delta t=5$, 100,000 source particles, 200 cells

Table 3. Relative RMS errors for Su-Olson problem, coarse timesteps, $\Delta t=5$, 100,000 source particles, 200 cells

Time	Relative RMS Error in I (%)					Relative RMS Error in Ur (%)				
	AMCE	AMCI	CF	AL	IMC, $\alpha=0.5$	AMCE	AMCI	CF	AL	IMC, $\alpha=0.5$
0.1	1.9	2.5	1.9	3.8	2.4	23.	16.	7.9	26.	15.
0.316	1.8	1.9	3.2	1.5	2.7	8.6	2.7	5.9	6.3	7.8
1.0	1.7	1.6	1.1	1.1	1.0	4.8	2.3	1.4	2.3	2.3
3.16	6.0	3.9	1.2	0.85	1.9	8.7	5.3	0.54	1.0	1.7
10.0	3.9	0.99	0.70	0.56	0.42	8.8	0.90	0.41	0.66	0.63
31.6	2.0	0.96	0.73	0.69	1.1	14.	0.87	0.57	0.61	0.58
100.0	4.4	1.6	0.68	0.94	0.72	11.	0.74	1.3	0.83	1.1
CPU time	182	117	116	110	128					